Provided for non-commercial research and education use.
Not for reproduction, distribution or commercial use.

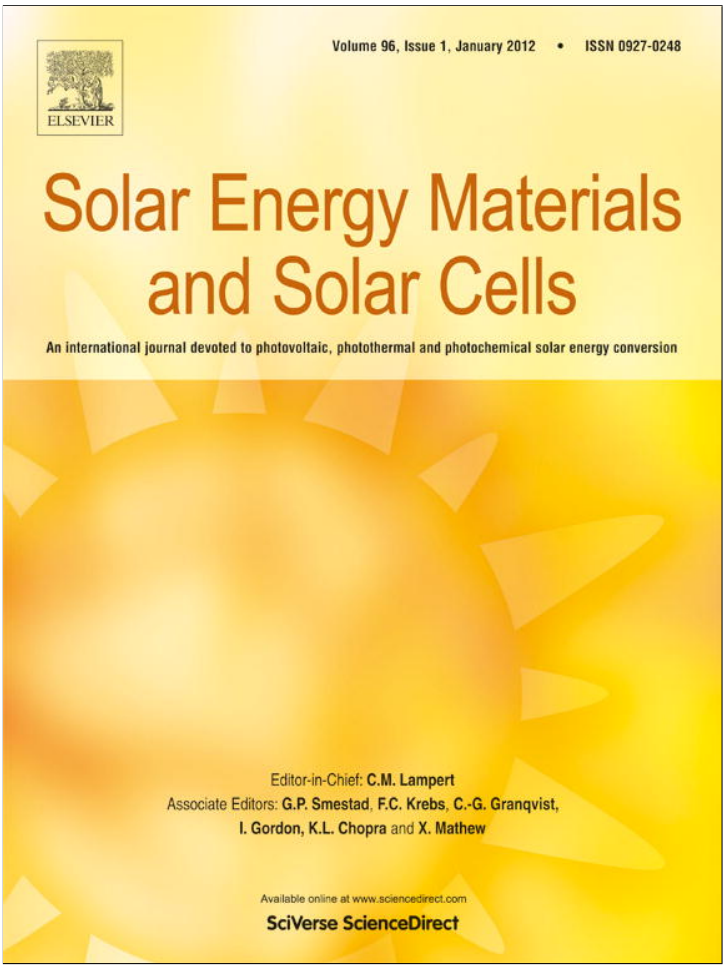

This article appeared in a journal published by Elsevier. The attached copy is furnished to the author for internal non-commercial research and education use, including for instruction at the authors institution and sharing with colleagues.

Other uses, including reproduction and distribution, or selling or licensing copies, or posting to personal, institutional or third party websites are prohibited.

In most cases authors are permitted to post their version of the article (e.g. in Word or Tex form) to their personal website or institutional repository. Authors requiring further information regarding Elsevier's archiving and manuscript policies are encouraged to visit:

http://www.elsevier.com/copyright

Author's personal copy

Solar Energy Materials & Solar Cells 96 (2012) 137–140

Contents lists available at SciVerse ScienceDirect

Solar Energy Materials & Solar Cells

journal homepage: www.elsevier.com/locate/solmat

Spray-coated ZnO electron transport layer for air-stable inverted organic solar cells

Yong-Jin Kang [a,b], Kyounga Lim [a], Sunghoon Jung [a], Do-Geun Kim [a], Jong-Kuk Kim [a], Chang-Su Kim [a], Soo H. Kim [b,*], Jae-Wook Kang [a,**]

[a] Department of Material Processing, Korea Institute of Materials Science (KIMS), Changwon 641-831, Republic of Korea
[b] Department of Nanosystem and Nanoprocess Engineering, Pusan National University, Busan 609-735, Republic of Korea

ARTICLE INFO

Article history:
Received 6 July 2011
Received in revised form
14 September 2011
Accepted 17 September 2011
Available online 14 October 2011

Keywords:
Spray coating
Organic solar cell
ZnO
Air stable

ABSTRACT

This study evaluated the possibility of utilizing a spray-coating process for inverted organic solar cells (IOSCs). The performance and stability of the IOSCs with zinc oxide (ZnO) as the electron transport layer made by different processes, such as spray-coating, spin-coating and sputtering, were investigated. The IOSCs subjected to the spray-coated ZnO layer showed a power conversion efficiency of $3.17 \pm 0.11\%$ under AM 1.5 simulated illumination and stability ($> 80\%$ of its original efficiency after 30 days). The device performance and stability of the IOSCs with the spray-coated ZnO layer was compared with those of spin-coated and sputtering deposited layers.

© 2011 Elsevier B.V. All rights reserved.

1. Introduction

Organic solar cell (OSC) has emerged as one of the promising photovoltaic devices because it can be manufactured cost effectively and is compatible with flexible substrates [1–5]. In addition, the relatively low power conversion efficiency (PCE) of OSCs has improved significantly over the last decade. Many research groups reported that polymer solar cells based on poly(3-hexylthiophene) (P3HT) and (6,6)-phenyl-C61 butyric acid methyl ester (PCBM) blends showed a PCE of ~5% [6–8]. Recently, a maximum PCE of $8.3 \pm 0.3\%$ was measured at the National Renewable Energy Laboratory for a cell area of 1.031 cm^2 fabricated by Konarka Technologies, Inc. [9]. On the other hand, these studies were performed using a spin-coating process, which is not an ideal process for large-area and low-cost production of OSCs. The fabrication of large-scale and solution processable OSCs requires scalable methods of device processing showing a large-area coating with high device efficiency.

A range of methods have been used to fabricate OSCs including spin-coating [4–10], spray-coating [3,11–16], inkjet-printing [17–20] and screen printing [21–23]. Among the various techniques, spin-coating is used widely because of the good uniformity of the deposited film and simple process. However, it is incompatible with large-area processes or flexible substrates. A spray-coating process with potential advantages of enabling a large-area coating and low-cost manufacturing can be a promising substitute for overcoming the drawbacks of the spin-coating process [3,12,13]. Many research groups have focused on controlling the surface roughness and coating thickness of the active layer and even the metal electrode in the OSCs [13,24].

Unlike conventional OSCs, inverted OSCs (IOSCs) have attracted attention recently [5,25–28]. The advantage of IOSCs is that it has a long life-time without a critical degradation of PCE because the Ag anode has better oxidation resistance than the Al cathode in conventional OSCs [5,28]. In IOSCs, zinc oxide (ZnO) is one of the most widely studied materials owing to its promising optical, electrical and optoelectronic properties. The formation of a ZnO interfacial layer between the active layer and ITO electrode in IOSCs is an important process for enhancing the selectivity of contact. The PCE of IOSCs with a spin-coated ZnO layer was reported to be as high as 2.5–3.5% [26,28].

This paper reports the fabrication of IOSCs with a ITO/ZnO/P3HT–PCBM/PEDOT–PSS/Ag structure utilizing a spray-coated ZnO electron transport layer. The effects of the spray-coated ZnO layer on the device performance and life time enhancements were investigated under a range of conditions (annealing temperature and thickness), and the performance of the IOSCs with the spray-coated ZnO layer was then compared with that of the spin-coated and sputtering deposited layers.

2. Experimental details

To fabricate an OSC, the ITO substrate with a sheet resistance of ~10 Ω/sq first underwent a routine cleaning procedure, which

* Corresponding author. Tel.: +82 55 350 5287; fax: +82 55 350 5653.
** Corresponding author. Tel.: +82 55 280 3572; fax: +82 55 280 3570.
E-mail addresses: sookim@pusan.ac.kr (S.H. Kim), jwkang@kims.re.kr (J.-W. Kang).

0927-0248/$ - see front matter © 2011 Elsevier B.V. All rights reserved.
doi:10.1016/j.solmat.2011.09.045

Author's personal copy

included sonication and repeated rinsing in acetone and isopropyl alcohol. The substrates were then dried in an oven and treated with UV–ozone for 5 min. The ZnO sol–gel solution was prepared using zinc acetate (16.40 mg, Aldrich) dissolved in 2-methoxyethanol (100 ml, Aldrich) using a magnetic stirrer. Ethanolamine (5 ml, Aldrich) was then added and the resulting solution was kept at 60 °C for 1 h under ambient conditions with vigorous stirring. Before spray-coating, the ZnO solution was diluted with methanol (ZnO sol–gel:methanol=1:10) because a solution without dilution was not well distributed from the nozzle or the layer was not coated uniformly. The spray-coating conditions were optimized to minimize the surface roughness by varying the solution injection rate, carrier gas flow, nozzle–substrate distance and printing speed.

The ZnO thin film was also prepared by RF magnetron sputtering using a 4-in. ZnO target with 99.99% purity. ITO or the glass substrate was placed at a distance of 13 cm from the target. Sputtering was carried out at a pressure of 0.24 mTorr with a sputtering power of 100 W for 10 min, resulting in a growth rate of 4 nm/min. Pure argon gas was used as the sputtering gas.

The poly(3-hexylthiophene) (P3HT):[6,6]-phenyl-C61 butyric acid methyl ester (PCBM) blend solution was prepared at a 1:1 mass ratio in 1,2-dichlorobenzene (20 mg/ml P3HT and 20 mg/ml PCBM). The active material was then coated on the ZnO layer with an average thickness of ~250 nm using a spin-coating process (with a spin speed of 600 rpm for 40 s) in a glove box. Subsequently, a solvent evaporation was performed for 2 h and pre-annealing was carried out at 150 °C for 20 min in a glove box. A buffer layer of poly (3,4-ethylenedioxylenethiophene) (PEDOT–PSS, Baytron P):isopropyl alcohol (IPA) (PEDOT–PSS:IPA=1:2) was prepared using a spin coater after passing through a 0.45 μm filter with a thickness of approximately 40 nm. The coated PEDOT–PSS film was dried at 150 °C for 1 min on a hot plate in a glove box. Finally, a 120 nm-thick Ag electrode was deposited on the PEDOT–PSS layer by thermal evaporation at 3×10^{-6} Torr. The effective area of the active layer for the solar cell prepared in this approach was 0.38 cm^2, which was determined using a shadow mask. The current density–voltage (*J–V*) characteristics of the IOSC were measured under AM 1.5 simulated illumination with an intensity of 100 mW/cm^2 (Pecell Technologies Inc., PEC-L11). The intensity of sunlight illumination was calibrated using a standard Si photodiode detector with a KG-5 filter [3,10]. The *J–V* curves were recorded automatically using a Keithley SMU 2410 source meter by illuminating the IOSC prepared.

3. Results and discussion

Fig. 1 shows a schematic diagram of the spray-coating process apparatus for the ZnO layer. The spray-coating system has two nozzles as the core and the clad [3]. The core nozzle was connected to the calibrated syringe injection pump for the ZnO sol–gel solution and the clad nozzle was linked to N_2 for the carrier gas. A computer controlled *xy* stage (nozzle and substrate moving stage) and injection pump allows a reproducible process. The ZnO coating conditions were optimized to minimize the surface roughness.

Fig. 2 shows that the thickness of the ZnO layer depends strongly on the injection rate at a constant gas pressure (50 psi), the spray nozzle–substrate distance (8.5 cm) and the printing speed (6 cm/min at substrate and 1800 cm/min at nozzle direction). With a single pass spray-coating process (single pass to substrate trajectory), it was possible to produce a ZnO thin film reproducibly with a thickness ranging from 15 to 25 nm. The coated ZnO layer was annealed thermally at 300 °C for 10 min under atmospheric conditions. The 40 nm thick spin-coated (with a spin speed of 3000 rpm for 40 s) and spray-coated films (with a two-pass spray-coating process) were characterized by atomic force microscopy (AFM), as shown in the inset in Fig. 2. The

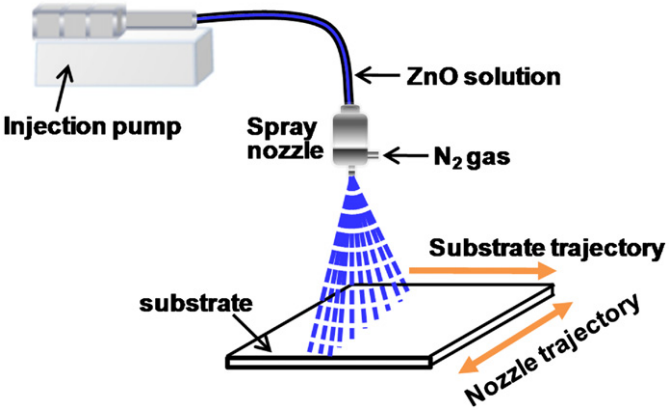

Fig. 1. Schematic diagram of the spray-coating apparatus.

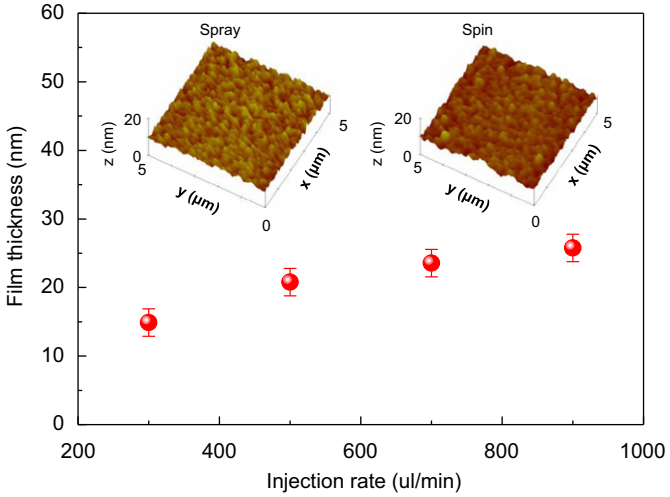

Fig. 2. Thickness of the spray-coated ZnO layer as a function of the injection rate with a constant air pressure of 50 psi, nozzle–substrate distance of 8.5 cm and printing speed of 6 cm/min along the *x*-axis and 1800 cm/min along the *y*-axis. Inset: AFM images of the spin- and spray-coated ZnO layer with a thickness of 40 nm.

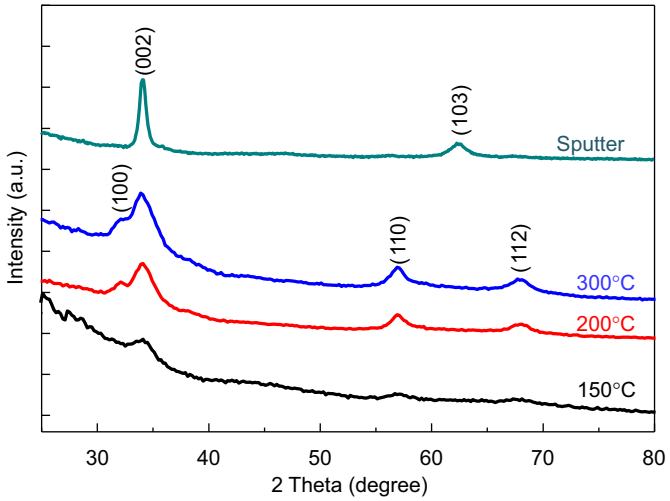

Fig. 3. X-ray diffraction pattern of ZnO films coated on a glass substrate by a spray-coating process at three different annealing temperatures, and deposited by sputtering at RT.

Author's personal copy

Table 1
Summary of the IOSC performance with the spin-coated, spray-coated and sputter-deposited ZnO electron transport layer with a 40 nm thickness. (Total of 30 devices were fabricated in several independent batches.)

Coating method	Annealing temperature (°C)	J_{sc} (mA/cm^2)	V_{oc} (V)	FF	PCE (%)	Rs (Ω cm^2)
Spin	150	8.28 ± 0.31	0.51 ± 0.004	0.38 ± 0.024	1.66 ± 0.21	8.74 ± 0.21
Spin	200	8.79 ± 0.28	0.57 ± 0.005	0.55 ± 0.007	2.83 ± 0.10	5.14 ± 0.16
Spin	300	9.62 ± 0.22	0.58 ± 0.005	0.55 ± 0.016	3.12 ± 0.07	4.31 ± 0.08
Spray	200	9.07 ± 0.34	0.59 ± 0.004	0.50 ± 0.02	2.71 ± 0.15	5.53 ± 0.13
Spray	300	9.62 ± 0.25	0.60 ± 0.004	0.55 ± 0.012	3.17 ± 0.11	4.56 ± 0.11
Sputter	–	10.02 ± 0.19	0.60 ± 0.005	0.53 ± 0.035	3.15 ± 0.17	4.71 ± 0.13

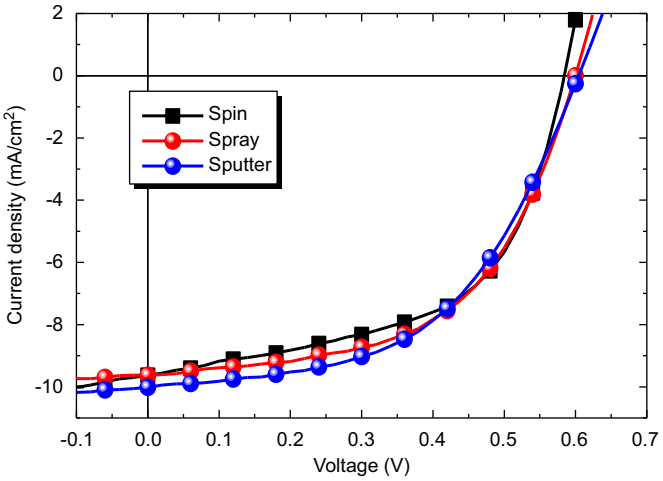

Fig. 4. Current density vs. voltage (J–V) characteristics of IOSCs fabricated with the spin-coated, spray-coated and sputtering deposited ZnO layer in ITO/ZnO(40 nm)/P3HT:PCBM(250 nm)/PEDOT–PSS(40 nm)/Ag devices. Spin- and spray-coated ZnO layers were annealed at 300 °C.

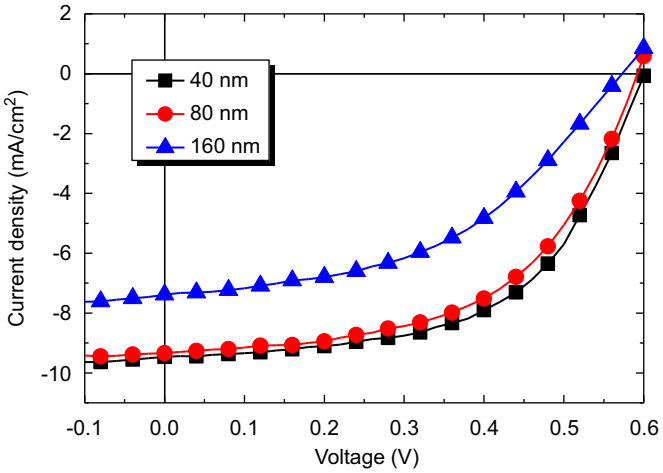

Fig. 5. Current density vs. voltage (J–V) characteristics of the IOSCs fabricated with the spray-coated ZnO layer with three different thicknesses.

optimized spray-coated ZnO film showed similar surface roughness to that of the the spin-coated layer with a root mean square (rms) roughness of 0.77 and 0.82 nm, respectively. This suggests that the spray-coating process can be replaced by spin-coating for ZnO layer deposition on a given substrate in terms of the morphology and film quality.

Fig. 3 shows the X-ray diffraction (XRD) patterns of the spray-coated ZnO films after thermal annealing from 150 to 300 °C and sputter deposited ZnO. When the annealing temperature was > 200 °C, the films showed (100) and (002) peaks at 32.1° and 33.9°, respectively, indicating that they were well-crystallized. The sputter deposited ZnO films showed a sharp diffraction peak of (002), indicating that this film was highly c-axis oriented.

The effect of the annealing temperature of the ZnO electron transport layer on the device performance was investigated, as shown in Table 1. With increasing annealing temperature, the PCE of the IOSCs with the spin-coated ZnO layer was improved from 1.66 to 3.12%. The series resistance (Rs) from the inverse slope of the J–V curve at J=0 decreased significantly from 8.74 to 4.31 Ω cm^2 with increasing annealing temperature, resulting from an increase in the crystallinity of the ZnO layer after thermal annealing (as shown in Fig. 3). Moreover, the devices with the spin- and spray-coated ZnO layer annealed at 300 °C showed better overall performance than those with annealing at 200 °C.

Fig. 4 presents the J–V characteristics of the spin-coated, spray-coated and sputtering deposited ZnO based IOSCs. The IOSCs with the spray-coated ZnO layer with a cell area of 0.38 cm^2 showed a short circuit current density (J_{sc}) of 9.62 mA/cm^2, an open circuit voltage (V_{oc}) of 0.60 V, a fill factor (FF) of 0.55 and a PCE of 3.17%. These results are comparable to those with the spin-coated

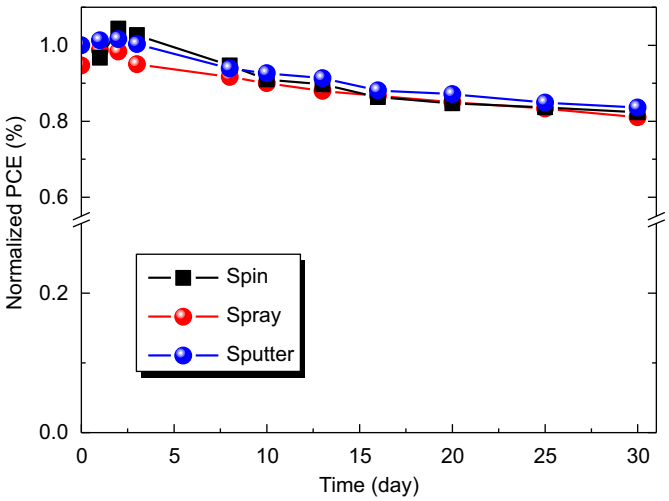

Fig. 6. Normalized PCE of the unencapsulated IOSCs stored for 30 days in air under ambient conditions.

(J_{sc}=9.62 mA/cm^2, V_{oc}=0.58 V, FF=0.55 and PCE=3.12%) and sputtering deposited (J_{sc}=10.02 mA/cm^2, V_{oc}=0.60 V, FF=0.53 and PCE=3.15%) layers, which indicates that the spray-coating method can be used to evaluate the large-area IOSCs with high device performance.

Fig. 5 shows the photovoltaic response of the IOSCs produced with a different spray-coated ZnO thickness. The thickness of the ZnO layer in the IOSCs plays a major role in the device performance. With increasing ZnO thickness from 40 to 160 nm, the PCE of the IOSCs decreased dramatically from 3.17 to 1.97%, and the Rs

Author's personal copy

increased significantly from 4.48 to 6.78 Ωcm^2, resulting in a decrease in FF. When the ZnO layer was too thick (>80 nm), the J_{sc} decreased to 7.38 mA/cm^2 due to shadowing of the active layer. The 40 nm-thick ZnO layer showed optimal performance.

Fig. 6 shows the stability of the IOSCs with a ZnO layer prepared by spin-coating, spray-coating and sputtering processes. The stability studies were performed in the dark with ambient conditions tested according to ISOS-D-1(shelf) [29]. The performance of the IOSCs was evaluated for 30 days. The normalized PCE of the unencapsulated IOSCs with the spray-coated ZnO layer after 30 days showed a similar value of ~80% with the spin-coated and sputtered devices.

4. Conclusions

This study demonstrates that the spray-coating process is an alternative to replace the spin-coating and sputtering process for the ZnO electron transport layer in IOSCs. The surface roughness of the spray-coated ZnO layer can be controlled as a standard of the spin-coated surface. The unencapsulated IOSCs with the spray-coated ZnO layer showed a PCE of 3.17% and stability (>80% of its original efficiency after 30 days), which were similar to those of the devices using the spin-coated and sputtered layers. With further optimization, all-spray deposited IOSCs may become a reality in the near future for low-cost and roll-to-roll manufacturing.

Acknowledgements

This study was supported by the New and Renewable Energy of the Korea Institute of Energy Technology Evaluation and Planning (KETEP) (Grant no. 20103020010050) funded by the Ministry of the Knowledge Economy, Republic of Korea.

References

[1] M. Manceau, D. Angmo, M. Jorgensen, F.C. Krebs, ITO-free flexible polymer solar cells: from small model devices to roll-to-roll processed large modules, Organic Electronics 12 (2011) 566–574.
[2] A.J. Medford, M.R. Lilliedal, M. Jørgensen, D. Aarø, H. Pakalski, J. Fyenbo, F.C. Krebs, Grid-connected polymer solar panels: initial considerations of cost, lifetime and practicality, Optics Express 18 (2010) A272–A285.
[3] S.-Y. Park, Y.-J. Kang, S. Lee, D.-G. Kim, J.-K. Kim, J.-H. Kim, J.-W. Kang, Spray-coated organic solar cell with large-area of 12.25 cm^2, Solar Energy Materials and Solar Cells 95 (2011) 852–855.
[4] B.C. Thompson, J.M.J. Fréchet, Polymer–fullerene composite solar cells, Angewandte Chemie International Edition 47 (2008) 58–77.
[5] H.-L. Yip, S.K. Hau, N.S. Baek, A.K.-Y. Jen, Self-assembled monolayer modified ZnO/metal bilayer cathodes for polymer/fullerene bulk-heterojunction solar cells, Applied Physics Letters 92 (2008) 193313-1–193313-3.
[6] G. Dennler, M.C. Scharber, C.J. Brabec, Polymer–fullerene bulk-heterojunction solar cells, Advanced Materials 21 (2009) 1323–1338.
[7] W.-I. Jeong, J. Lee, S.-Y. Park, J.-W. Kang, J.-J. Kim, Reduction of collection efficiency of charge carriers with increasing cell size in polymer bulk heterojunction solar cells, Advanced Functional Materials 21 (2011) 343–347.
[8] Y. Liang, Y. Wu, D. Feng, S.T. Tsai, H.J. Son, G. Li, L. Yu, Development of new semiconducting polymers for high performance solar cells, Journal of the American Chemical Society 131 (2009) 56–57.
[9] 〈http://www.konarka.com/index.php/company/our-history/〉 (2010).
[10] S.-Y. Park, W.-I. Jeong, D.-G. Kim, J.-K. Kim, D.C. Lim, J.H. Kim, J.-J. Kim, J.-W. Kang, Large-area organic solar cells with metal subelectrode on indium tin oxide anode, Applied Physics Letters 96 (2010) 173301-1–173301-3.
[11] R. Green, A. Morfa, A.J. Ferguson, N. Kopidakis, G. Rumbles, S.E. Shaheen, Performance of bulk heterojunction photovoltaic devices prepared by airbrush spray deposition, Applied Physics Letters 92 (2008) 033301-1–1-033301-3.
[12] S.-I. Na, B.-K. Yu, S.-S. Kim, D. Vak, T.-S. Kim, J.-S. Yeo, D.-Y. Kim, Fully spray-coated ITO-free organic solar cells for low-cost power generation, Solar Energy Materials and Solar Cells 93 (2010) 1333–1337.
[13] C. Girotto, D. Moia, B.P. Rand, P. Heremans, High-performance organic solar cells with spray coated hole-transport and active layer, Advanced Functional Materials 21 (2011) 64–72.
[14] C.N. Hoth, R. Steim, P. Schilinsky, S.A. Choulis, S.F. Tedde, O. Hayden, C.J. Brabec, Topographical and morphological aspects of spray coated organic photovoltaics, Organic Electronics 10 (2009) 587–593.
[15] K.X. Steirer, M.O. Reese, B.L. Rupert, N. Kopidakis, D.C. Olson, R.T. Collins, D.S. Ginley, Ultrasonic spray deposition for production of organic solar cells, Sol. Energy Materials and Solar Cells 93 (2009) 447–453.
[16] J. Weickert, H. Sun, C. Palumbiny, H.C. Hesse, L. Schmidt-Mende, Spray-deposited PEDOT–PSS for inverted organic solar cells, Solar Energy Materials and Solar Cells 94 (2010) 2371–2374.
[17] S.H. Eom, S. Senthilarasu, A.P. Uthirakumar, S.C. Yoon, J. Lim, C. Lee, H.S. Lim, S.H. Lee, Preparation and characterization of nano-scale ZnO as a buffer layer for inkjet printing of silver cathode in polymer solar cells, Solar Energy Materials and Solar Cells 92 (2008) 564–570.
[18] T. Aernouts, T. Aleksandrov, C. Girotto, J. Genoe, J. Poortmans, Polymer based organic solar cells using ink-jet printed active layer, Applied Physics Letters 92 (2008) 033306-1–033306-3.
[19] A. Teichler, R. Eckardt, S. Hoeppener, C. Friebe, J. Perelaer, A. Senes, M. Morana, C.J. Brabec, U.S. Schubert, Combinatorial screening of polymer:-fullerene blends for organic solar cells by inkjet printing, Advanced Energy Materials 1 (2011) 105–114.
[20] V. Marin, E. Holder, M.M. Wienk, E. Tekin, D. Kozodaev, U.S. Schubert, Ink-jet printing of electron donor/acceptor blends: towards bulk heterojunction solar cells, Macromolecular Rapid Communications 26 (2005) 319–324.
[21] S.E. Shaheen, R. Radspinner, N. Peyhambarian, G.E. Jabbour, Fabrication of bulk heterojunction plastic solar cells by screen printing, Applied Physics Letters 79 (2001) 2996–2998.
[22] F.C. Krebs, Polymer solar cell modules prepared using roll-to-roll methods: knife-over-edge coating, slot-die coating and screen printing, Solar Energy Materials and Solar Cells 93 (2009) 465–475.
[23] F.C. Krebs, M. Jorgensen, K. Norrman, O. Hagemann, J. Alstrup, T.D. Nielsen, J. Fyenbo, K. Larsen, J. Kristensen, A complete process for production of flexible large area polymer solar cells entirely using screen printing—first public demonstration, Solar Energy Materials and Solar Cells 93 (2009) 422–441.
[24] C. Girotto, B.P. Rand, S. Steudel, J. Genoe, P. Heremans, Nanopaticle-based, spray-coated silver top contacts for efficient polymer solar cells, Organic Electronics 10 (2009) 735–740.
[25] F. Zhang, X. Xu, W. Tang, J. Zhang, Z. Zhuo, J. Wang, J. Wang, Z. Xu, Y. Wang, Recent development of the inverted configuration organic solar cells, Solar Energy Materials and Solar Cells 95 (2011) 1785–1799.
[26] M.S. White, D.C. Olson, S.E. Shaheen, N. Kopidakis, D.S. Ginley, Inverted bulk-heterojunction organic photovoltaic device using a solution-derived ZnO underlayer, Applied Physics Letters 89 (2006) 143517-1–143517-3.
[27] K. Norrman, M.V. Madsen, S.A. Gevorgyan, F.C. Krebs, Degradation patterns in water and oxygen of an inverted polymer solar cell, Journal of the American Chemical Society 132 (2010) 16883–16892.
[28] S.K. Hau, H.-L. Yip, K. Leong, A.K.-Y. Jen, Spraycoating of silver nanoparticle electrodes for inverted polymer solar cells, Organic Electronics 10 (2009) 719–723.
[29] M.O. Reese, S.A. Gevorgyan, M. Jørgensen, E. Bundgaard, S.R. Kurtz, D.S. Ginley, D.C. Olson, M.T. Lloyd, P. Morvillo, E.A. Katz, A. Elschner, O. Haillant, T.R. Currier, V. Shrotriya, M. Hermenau, M. Riede, K.R. Kirov, G. Trimmel, T. Rath, O. Inganas, F. Zhang, M. Andersson, K. Tvingstedt, M. Lira-Cantu, D. Laird, C. McGuiness, S.J. Gowrisanker, M. Pannone, M. Xiao, J. Hauch, R. Steim, D.M. DeLongchamp, Roland Rösch, H. Hoppe, N. Espinosa, A. Urbina, G. Yaman-Uzunoglu, J.-B. Bonekamp, A.J.J.M. van Breemen, C. Girotto, E. Voroshazi, F.C. Krebs, Consensus stability testing protocols for organic photovoltaic materials and devices, Solar Energy Materials and Solar Cells 95 (2011) 1253–1267.